RAPID COMMUNICATIONS IN MASS SPECTROMETRY, VOL. **11**, 484–488 (1997)

Matrix-assisted Laser Desorption/Ionization by Two Collinear Subthreshold Laser Pulses

Xiaodong Tang, Mehrnoosh Sadeghi, Zohra Olumee and Akos Vertes*

Department of Chemistry, George Washington University, Washington, DC 20052, USA

SPONSOR REFEREE: Professor Kenneth G. Standing, Physics Department, University of Manitoba, Winnipeg, MB, R3T 2N2, Canada

Two nitrogen laser pulses of subthreshold irradiance were used to achieve matrix-assisted laser desorption/ionization in a collinear configuration. Optimum laser pulse delay times yielding maximum guest ion intensities were determined for four different matrices between 4.2 ns for sinapinic acid (SA) and 12.5 ns for 2,5-dihydroxybenzoic acid (DHB). The signal decay times followed an opposite trend to the position of maxima, DHB being the fastest decaying (1.1 ns) and SA the slowest (9.8 ns). Collinear subthreshold experiments allow for a two orders of magnitude improvement in spatial and time resolution over post-ionization experiments. © 1997 by John Wiley & Sons, Ltd.

Received 18 January 1997; Accepted 19 January 1997
Rapid. Commun. Mass Spectrom. **11**, 484–488 (1997)
No. of Figures: 4 No. of Tables: 1 No. of Refs: 14

There is a widening gap between the fast growing practical importance of matrix-assisted laser desorption/ionization (MALDI) and the limited understanding of basic processes involved. Fundamental studies of MALDI have typically focused on the laser fluence dependence of neutral and ion yields[1–3] and on the velocity distributions of desorbed particles.[4,5] These measurements led to the understanding that threshold laser irradiances exist for both neutral and ionized particles. The desorption of neutrals exhibits a lower threshold (e.g. $\sim 4 \times 10^5$ W/cm^2 in Ref. 1) than the generation of ions (e.g. $\sim 2 \times 10^6$ W/cm^2 in Ref. 1). For ions, the definition of threshold is based on achieving a certain signal-to-noise (S/N) ratio (typically S/N $\approx$ 2) for the guest molecular ions in the mass spectrum.[3] Analysis of the pulse-height distributions in single-ion counting experiments indicates that MALDI relies on a phase-transition-like collective process.[2] Velocity distributions of ionized guest molecules show little or no dependence on the mass of the guest molecules.[4] Although the actual velocities determined in different experiments are different for neutrals (e.g. $\sim$350 m/s for ferulic acid molecules[5]) and for ions (e.g. $\sim$1140 m/s for sinapinic acid (SA) ions[4]), mass-independent guest velocities point to jet expansion as the likely accelerating mechanism for guest particles. Hydrodynamic expansion studies[6] and molecular dynamics calculations[7] indicate similar lift-off velocities for neutrals and the possible role of expansion cooling in the stabilization of guest particles.

Simultaneous detection of ions and neutrals in the MALDI process shows that in the vicinity of the ion formation threshold, the degree of ionization for guest particles is of the order of 0.01%.[8] In order to measure ion yields and neutral velocities, several investigators used 'post-ionization' experiments.[1,3,5,8] In these experiments, two laser pulses were used in a cross-beam configuration. The first laser beam was focused on the sample surface at $\sim$45°, whereas the second laser was aligned parallel with the sample surface at a given distance in order to intercept and ionize the desorbed neutrals. The post-ionization laser typically had a shorter wavelength (e.g. 118 nm,[5] 128.1 nm[8] and 248 nm[3]) and a higher intensity for efficient photoionization.

Our objective was to explore the subthreshold processes involved in MALDI. By using two collinear subthreshold laser pulses with variable delay time between them, we wanted to uncover how the MALDI signal depended on the processes initiated by the first pulse. The term 'subthreshold' meant that the individual laser pulses did not lead to ion formation, i.e. their intensity was below the ion formation threshold, $I_{\mathrm{thr,ion}}$. We assumed that the combination of two pulses at $\sim 0.6 I_{\mathrm{thr,ion}}$ with no time delay between the pulses led to $\sim 1.2 I_{\mathrm{thr,ion}}$ and an observable MALDI signal. We also expected that no delay between the pulses would result in the maximum MALDI signal and an increasing delay time would lead to gradual decay of the signal. This scenario could have been an indication of solid-state excited-state control. As it turned out, the results did not support our original expectations.

It is important to emphasize the conceptual difference between the present study and the post-ionization experiments. In our investigations both lasers were working at the same wavelength (337 nm); thus, neither of them had enhanced ionization capability. Also, the collinear laser geometry allowed for the illumination of the same volume at the sample surface for both lasers. The crossed-beam geometry in post-ionization experiments resulted in a separate desorption volume at the sample surface and ionization volume at the plume/ionizing beam intercept.

EXPERIMENTAL

Instrumentation

MALDI experiments were carried out on a linear time-of-flight mass spectrometer (TOF 101, Comstock, Oak Ridge, TN, USA) with a laser desorption source described in detail elsewhere.[9] As shown in Fig. 1, the original arrangement was modified by adding a second

*Correspondence to: A. Vertes
Contract grant sponsor: National Science Foundation; Contract grant number: CTS-9212389

CCC 0951–4198/97/050484–05 $17.50

sealed-cartridge nitrogen laser source (VSL-337ND, Laser Science, Newton, MA, USA) providing excitation at λ = 337 nm. The energies of laser I and laser II, as measured with a pyroelectric joule meter (J4-05, Molectron Detector, Portland, OR, USA), were 250 ± 4 and 320 ± 5 μJ per pulse, respectively. The approximate focal spot diameter, $d \approx 100$ μm, was measured using photographic paper. Both laser pulse widths were determined by a fast photodiode (DET2-SI, Thorlabs, Newton, NJ, USA) to be 5 ± 0.5 ns full width at half maximum (FWHM). The recharge time for the plasma cartridges of the nitrogen lasers was found to be 521 ± 4 ns for laser I and 482 ± 5 ns for laser II.

A 30% transmission, 15% reflection beamsplitter (Esco, Oak Ridge, NJ, USA) was used to combine the two beams. Because collinearity was critical for the excitation of the same sample spot, light paths and beam cross-sections were carefully verified along the optical path. The overlap of focal spots was also checked by exposure of photographic paper attached to the probe surface. The alignment was considered satisfactory when the two traces of the focal spots were indistinguishable. Multiple shot marks on the photographic paper also indicated acceptable directional stability of the lasers. Because we wanted to achieve comparable final intensities for the two pulses, a 56% transmission neutral density filter was mounted in front of laser I. A single variable attenuator (935-3-OPT, Newport, Fountain Valley, CA, USA) was used to control both fluences. In the collinear region after the beam splitter, the energy ratio of laser I to laser II was 0.88:1.

Tight control of laser fluences was necessary to maintain subthreshold excitation. First the ionization threshold irradiance, $I_{thr,ion}$, was measured for every guest molecule/matrix combination, then the laser energies were adjusted accordingly. As in other studies, the definition of ionization threshold was based on the S/N ≈ 2 criterion. The subthreshold nature of laser intensities was regularly confirmed by delivering individual pulses from the two lasers. At the appropriate attenuator setting, neither of the individual pulses led to detectable guest ion signals, whereas the combination of the two pulses with adequate delay resulted in non-zero guest ion currents.

The triggering events of the two lasers, and also of the oscilloscope and the transient recorder, were controlled by a digital delay generator (DG535, Stanford Research Systems, Sunnyvale, CA, USA). As shown in the inset of Fig. 1, the timing sequence followed the order laser I, laser II and oscilloscope/transient recorder. The oscilloscope and transient recorder were triggered 480 ns after laser I to compensate for most of the re-charge time of the two lasers. The actual time delay between the two laser pulses was altered by changing the delay setting for laser I in increments of 2.0 ns. We monitored the real time delay corresponding to each delay setting using the fast photodiode and a digital oscilloscope (TDS 320, Tektronix, Beaverton, OR, USA). Jitter values for the emissions of laser I and laser II were ± 4.2 and ± 4.8 ns, respectively. Thus, the uncertainty of delay time between the two pulses was ± 6.4 ns.

The laser-generated positive ions were accelerated from the probe tip at + 30.0 kV towards a grid kept at ground potential. After drifting in the 215 cm field-free region, the ions were detected by a dual multichannel plate assembly (Galileo Electro-Optics, Sturbridge, MA, USA) biased to –1900 V. A 120 MHz preamplifier (Model 9305, EG&G ORTEC, Oak Ridge, TN, USA) was followed by a variable gain amplifier module (Model 6103, LeCroy, Albuquerque, NM, USA) to extend the dynamic range of detection. A fast transient digitizer (TR8828D, LeCroy) recorded the ion current with 8-bit resolution. Data acquisition and initial data analysis were performed on a 486D/33 MHz personal computer using a custom software package (TOFWARE, Ilys Software, Pittsburgh, PA, USA).

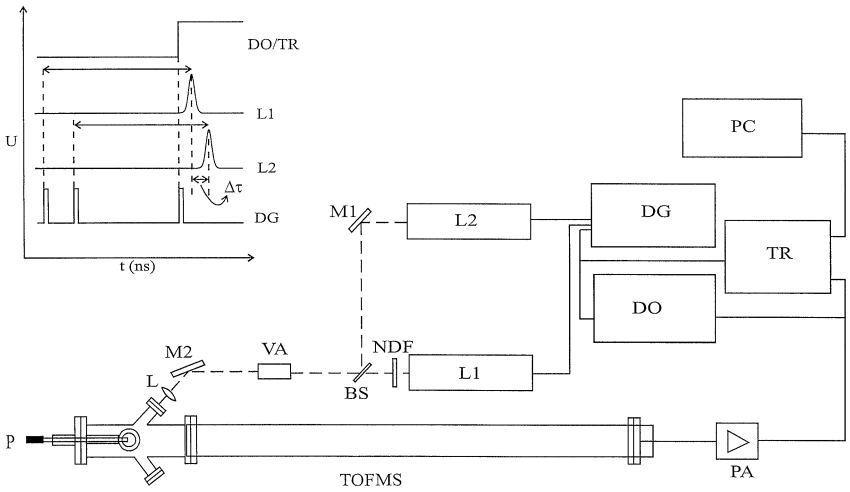

Figure 1. Schematic view of the experimental arrangement involving a time-of-flight mass spectrometer with two nitrogen laser sources. L1 = laser I; L2 = laser II; TR = transient recorder; DO = digital oscilloscope; DG = delay generator; M1 and M2 = mirrors; BS = beam splitter; NDF = neutral density filter; VA = variable attenuator; L = focusing lens; PA = preamplifier; PC = personal computer. The triggering sequence provided by the delay generator is presented in the inset (for description, see text).

Sample preparation

Bovine insulin (Sigma Chemical, St. Louis, MO, USA) and decathymidylic acid ($d(T)_{10}$) (Cruachem, Dulles, VA, USA) were chosen as model systems for guest molecules. The protein was embedded in one of the following matrices: 6-aza-2-thiothymine (ATT), 3,5-dimethoxy-4-hydroxycinnamic acid (sinapinic acid, SA) and 2,5-dihydroxybenzoic acid (DHB), whereas the oligonucleotide behavior was tested using a 3-hydroxypicolinic acid (3-HPA) matrix. ATT, SA and 3-HPA were purchased from Aldrich Chemical (Milwaukee, WI, USA). Prior to use, DHB (from Sigma) was recrystallized twice in order to remove excessive sodium salts present in the original product. All other matrices were used without purification.

The 5×10^{-4} M protein and oligonucleotide solutions were prepared in 0·1% trifluoroacetic acid (TFA). Saturated matrix solutions were made using 7:3 (v/v) acetonitrile + water (HPLC grade) solvent. For sample preparation, 10 µL of matrix solution were mixed with 2 µL of the guest solution to provide at least a 1000:1 matrix-to-guest molecule ratio. The mixture was dried in a stream of cold air prior to insertion into the ion source. For the experiments involving insulin, internal mass calibration was applied utilizing protein and matrix related ions. In the case of $d(T)_{10}$, bovine insulin was used as an external standard. The mass accuracy was within ±0.1% for external and ±0.05% for internal calibration.

Data acquisition and analysis

For each time-delay setting a total of 200 consecutive spectra were recorded from ~10 different spots on the sample surface. Spectra with overloaded matrix and/or guest ion peaks were discarded (this accounted for less than 5% of the total spectra). From the remaining data, 50 consecutive spectra were averaged to improve the signal-to-noise ratio. Baseline corrections were performed using windowed median and moving average filters.

The averaged raw flight time spectra were analyzed using the Origin scientific software package (Microcal Software, Northampton, MA, USA). Peak area measurements were performed by Lorentzian fit of guest ion-current data and integration of the best-fit curve. The Lorentzian fit was chosen over Gaussian because it seemed to approximate the peak shapes better in the high mass range. This may be attributed to the presence of unresolved isotopic and adduct ion peaks and also partial fragmentation of the guest molecules. The MALDI ion yields were plotted as a function of delay time.

Investigation of the ion yield curves revealed two important features in each plot. The first notable feature was the presence of a maximum at a non-zero delay time. In every experiment, the maximum was followed by a decay region that could be approximated by an exponential decay. The delay time associated with the maximum guest ion yield and decay time constants were obtained by a least-squares fit for each matrix–guest pair.

RESULTS AND DISCUSSION

Figure 2 shows the delay time dependence of insulin ion yield in an SA matrix. Vertical error bars represent the statistical error in the ion-current measurements, whereas horizontal bars correspond to the jitter in the actual delay times between the laser pulses. Maximum ion production is observed at t_{max} = 4.2 ns. This result disagrees with the intuitive assumption that two subthreshold pulses coming at the same time generate the largest number of ions. The existence of a finite optimum delay points to the presence of at least two consecutive subprocesses in MALDI (see discussion later). Following the maximum, a simple exponential decay fits the data reasonably well. The decay time for insulin at SA is t_{dec} = 9.8 ns.

A similar trend is observed in the case of $d(T)_{10}$ desorption from a 3-HPA matrix (see Fig. 3) with a later maximum, t_{max} = 8.1 ns, and a shorter decay time,

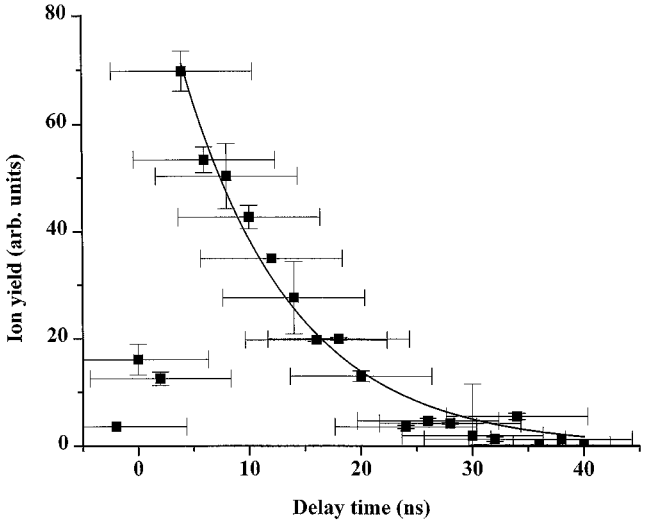

Figure 2. Desorbed ion yield of insulin guest molecules in an SA matrix as a function of delay time between two subthreshold laser pulses at 337 nm. The solid line represents the exponential decay determined by a least-squares fit (see text).

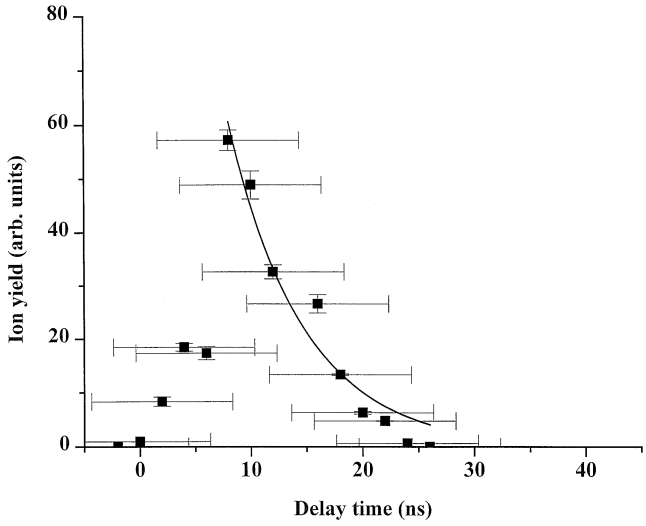

Figure 3. Positive ion yield of $d(T)_{10}$ guest molecules desorbed from a 3-HPA matrix at different triggering delays between the two laser pulses. The exponential decay least-squares fit is shown by the solid line (see text).

Table 1. Time position of maxima and decay times for ion yields

Matrix/guest	t_{max} (ns)	t_{dec} (ns)
DHB/insulin	12.5	1.1
ATT/insulin	8.7	3.7
SA/insulin	4.2	9.8
3-HPA/d(T)$_{10}$	8.1	6.7

t_{dec} = 6.7 ns. Variations of these two time parameters seem to depend on the nature of the matrix. Measured values for the different matrix–guest pairs are listed in Table 1. The DHB–insulin pair exhibited the latest maximum and the shortest decay time. In contrast, the SA–insulin pair has the earliest maximum and the longest decay time. The ATT–insulin combination represents the middle ground in both parameters.

In order to identify the physical quantities associated with the observed characteristic times, a simple model will be introduced. If the irradiance of the first laser pulse, I_1, is between the desorption threshold, $I_{thr,des}$, and the ionization threshold, i.e. $I_{thr,des} < I_1 < I_{thr,ion}$, a plume of neutrals is generated by the first pulse. Assuming that the plume expansion velocity, v_{exp}, is not very different from the group velocity, v_{group} one can calculate the size of the plume at the end of the observation period in our experiment. The reported neutral group velocities of ferulic acid and SA matrices are in the range from 350 m/s[5] to 500 m/s.[8] Calculating with the higher velocity, a plume size of 20 μm is expected at the longest delay (40 ns) between the two laser pulses. This means that at the arrival of the second pulse, the plume is still entirely inside the focal region (see Fig. 4(b)).

There are two important consequences of this simple picture. First, unlike in the post-ionization experiments, the t_{max} value in the subthreshold experiments is not determined by the group velocity (compare Fig. 4(a) and (b)). Second, the signal decay at larger delay times (t_{dec}) is not associated with the plume leaving the intercepting beam (laser II in Fig. 4(a)). Accordingly, the time scales of the subthreshold and post-ionization experiments are very different. In three of the post-ionization studies of interest[1,5,8] ~4 μs delays were applied for the optimum signal, whereas the longest delay in the present study was 40 ns. Thus the subthreshold method is capable of capturing up to ~100 times faster processes than its post-ionization counterpart.

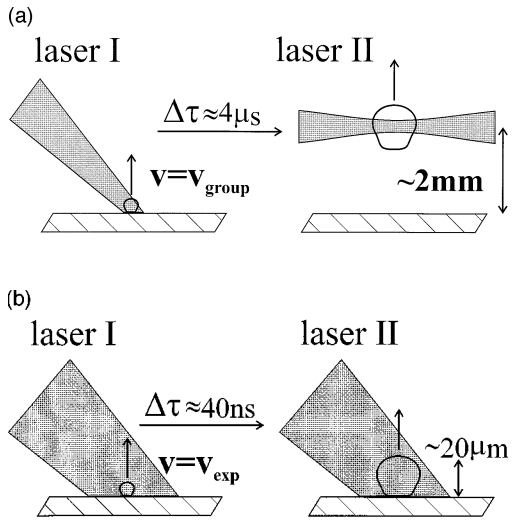

Figure 4. Comparison of the post-ionization and the subthreshold experiments. (a) Typical arrangement for postionization; (b) plume generation and expansion in the subthreshold experiment. Note that time scales and linear dimensions differ by two orders of magnitude.

With a minimum number of assumptions, we can attribute the presence and position of maximum yields to the production of guest ion precursors. When the concentration of these precursors is the maximum, the second laser pulse can convert them into ions with maximum efficiency. The production of available precursors can be regulated by the rate of the phase transition process, by the generation of excitons in the solid[10] or by the production of excited-state molecules in the plume. Similarly, the signal decay phase can be explained by invoking a number of processes. Among the most obvious possibilities are the radiative or collisional relaxation of excited-state molecules (matrix and/or guest). Moreover, if the expansion velocity is higher than the measured group velocities, the plume can expand beyond the interaction volume defined by the beam waist at the surface. In this situation, the signal decay can be attributed to the guest ion precursors leaving the interaction volume.

There is experimental evidence indicating that excited-state lifetimes can be very different for different matrices. Time-resolved laser-induced fluorescence measurements show that DHB has no long-lived excited states, whereas 3-HPA fluoresces for up to 100 μs.[10] Although 3-HPA shows a six times longer decay time (6.7 ns) in our subthreshold experiments than DHB (1.1 ns), these differences are clearly more modest than those observed in fluorescence lifetimes. This discrepancy may potentially argue against the role of excited matrix states in MALDI.[11,12]

Time-dependent quartz crystal microbalance measurements of the total yield reveal that the evaporation of the ferulic acid matrix continues for over 100 s after the laser pulse.[13] This extremely slow neutral-loss process would provide a continuous supply of plume material for the duration of both the post-ionization and the subthreshold experiments. This evidence for slow thermal desorption is hard to reconcile with either of the double-pulse experiments without assuming the active role of an excited species.

In the short delay time limit, the subthreshold experiments can also be viewed as a new way of probing the influence of laser pulse shape. It is known that, for certain proteins, pulses as short as 560 fs can be effective for MALDI.[14] These very short pulses represent a limiting case in terms of the plume dynamics. During the first few ps, the displacement of the surface molecules is only on the scale of a few nanometers. In other words, during this period no real plume formation can be observed; the sample surface is in the superheated liquid state. Therefore, the existence of an optimum pulse length in the picosecond regime cannot be observed. Systematic studies on the effect of pulse length and shape in the nanosecond regime, however, are not available. The presence of an ion yield maximum at finite delay times in this study supports the

idea of using laser pulses of extended but different duration for different matrix materials. Combination of laser pulses with selected properties and timing may pave the way for more efficient and flexible MALDI sources.

Acknowledgements

The authors are grateful for the financial support of the National Science Foundation (Grant No. CTS-9212389) for contributing towards the purchase of laser optics. They also express their appreciation to Laser Science for the loan of one of the nitrogen lasers used in this study. Two of the authors, M.S. and Z.O., were supported by fellowships and assistantships from George Washington University.

REFERENCES

1. B. Spengler, U. Bahr, M. Karas and F. Hillenkamp, *Anal. Instrum.* **17**, 173 (1988).
2. W. Ens, Y. Mao, F. Mayer and K. G. Standing, *Rapid Commun. Mass Spectrom.* **5**, 117 (1991).
3. K. Dreisewerd, M. Schürenberg, M. Karas and F. Hillenkamp, *Int. J. Mass Spectrom. Ion Processes* **141**, 127 (1995).
4. R. Beavis and B. Chait, *Chem. Phys. Lett.* **181**, 479 (1991).
5. T. Huth-Fehre and C. Becker, *Rapid Commun. Mass Spectrom.* **5**, 378 (1991).
6. A. Vertes, G. Irinyi and R. Gijbels, *Anal. Chem.* **65**, 2389 (1993).
7. A. Bencsura and A. Vertes, *Chem. Phys. Lett.* **247**, 142 (1995).
8. C. Mowry and M. Johnston, *Rapid Commun. Mass Spectrom.* **7**, 569 (1993).
9. Z. Olumee, M. Sadeghi, X. Tang and A. Vertes, *Rapid Commun. Mass Spectrom.* **9**, 744 (1995).
10. H. Ehring and B. U. R. Sundqvist, *J. Mass Spectrom.* **30**, 1303 (1995).
11. M. E. Gimon, L. M. Preston, T. Solouki, M. A. White, and D. H. Russell, *Org. Mass Spectrom.*, **27**, 827 (1992).
12. R. Knochenmuss, F. Dubois, M. J. Dale and R. Zenobi, in *Proceedings of the 44th Annual Conference on Mass Spectrometry and Allied Topics*, Portland, OR, 12–16 May, 1996, ASMS, Santa Fe, p. 732.
13. A. Quist, T. Huth-Fehre and B. U. R. Sundqvist, *Rapid Commun. Mass Spectrom.* **8**, 149 (1994).
14. P. Demirev, A. Westman, C. T. Reimann, P. Hakansson, D. Barofsky, B. U. R Sundqvist, Y. D. Cheng, W. Seibt and K. Siegbahn, *Rapid Commun. Mass Spectrom.* **6**, 187 (1992).

